

# FABRICATION, FIELD MEASUREMENT, AND TESTING OF A COMPACT RF DEFLECTING CAVITY FOR ELBE

Gowrishankar Thalagavadi Hallilingaiah<sup>\*, 1</sup>, André Arnold<sup>2</sup>, Sebastian Köppen<sup>2</sup>, Peter Michel<sup>1, 2</sup>, Ursula van Rienen<sup>1, 3</sup>

<sup>1</sup> University of Rostock, Rostock, Germany

<sup>2</sup> HZDR, Dresden, Germany

<sup>3</sup> Department Life, Light & Matter, University of Rostock, Rostock, Germany

## Abstract

A transverse deflecting cavity is being developed for the electron linac ELBE (Electron Linac for beams with high Brilliance and low Emittance) to separate the bunches into two or more beamlines so that multiple user experiments can be carried out simultaneously. A normal conducting double quarter-wave cavity has been designed to deliver a transverse kick of 300 kV when driven by an 800 W solid-state amplifier at 273 MHz. The main challenges in fabrication were machining the complex cavity parts with high precision, pre-tuning the cavity frequency, and the final vacuum brazing within the tolerances, which are described in this paper. The reason for a low intrinsic quality factor measured during the low power test was investigated, and suitable steps were taken to improve the quality factor. The cavity field profiles obtained from the bead-pull measurement matched the simulation results. Further, the cavity was driven up to 1 kW using a modified pick-up cup, and eventually, vacuum conditioning of the cavity was accomplished. The cavity fulfills the design requirements and is ready to be installed in the beamline.

## INTRODUCTION

The linear electron accelerator, ELBE (Electron Linac for beams with high Brilliance and low Emittance) at Helmholtz-Zentrum Dresden-Rossendorf (HZDR), Germany, is a versatile machine that drives six distinct secondary particle and radiation sources used in a wide range of experiments related to health, matter, transmutation, and accelerator development [1]. In the current beamline setup, the accelerated high energy beam can only be transported to a single experimental station at any given time. This limits the utilization of the accelerator to one user at a time. To overcome this limitation, a new radio-frequency (RF) deflecting cavity was proposed in [2], which can distribute the bunches from the existing single beam into two or more beamlines. This cavity would enable the simultaneous operation of the multiple downstream secondary sources, thus significantly enhancing the accelerator's capabilities. Furthermore, this deflecting cavity is being actively considered as a beam separator for the proposed future accelerator facility at HZDR [3]. The complete geometry of the deflecting cavity is shown in Fig. 1, and its parameters are listed in Table 1. The design of the cavity is discussed in [2], and this paper focuses on its fabri-

Table 1: Important Parameters of the Deflecting Cavity

Parameter	Value	Unit
Cavity: width x height x length	275x181x500	mm
Cavity aperture	$V_{ap}$	30 mm
Resonance frequency	$f_0$	273 MHz
Frequency tuning range	$\Delta f_0$	-1.67 to 1.86 MHz
Shunt impedance	$R_{\perp}/Q$	9.96 M $\Omega$
Intrinsic Q-factor	$Q_0$	11188
Geometry factor	$G$	57.03 $\Omega$
Deflecting voltage	$V_{\perp}$	300 kV
RF power loss	$P_0$	810 W
Peak electric field	$E_{pk}$	2.49 MV/m
Peak magnetic field	$S_{pk}$	1.21 W/cm <sup>2</sup>

cation. Additionally, we discuss the results of the frequency pre-tuning, on-axis field measurement and RF conditioning of the cavity.

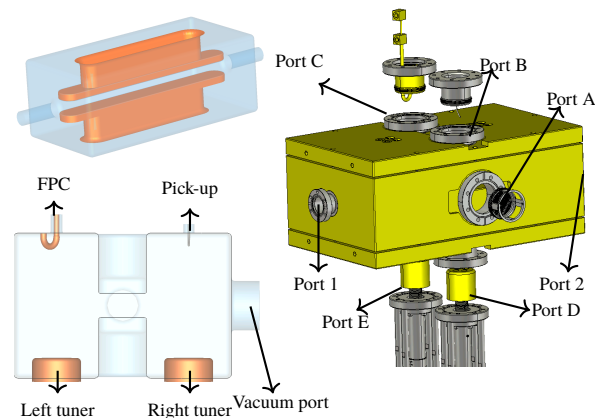


Figure 1: The cavity geometry showing all the cavity ports and the cavity components associated with the ports.

## FABRICATION

Manufacturing a cavity out of a single solid copper block is not viable, either technically or financially. The cavity must therefore be divided into smaller parts so that these parts can be machined with greater accuracy. However, the tolerances achieved during machining may be impacted by brazing since the number of brazing joints increases with the number of cavity parts. Therefore, the cavity should be divided into fewer parts to reduce the number of brazing joints while maintaining the required tolerances. The cavity

\* gowrishankar.hallilingaiah@uni-rostock.de

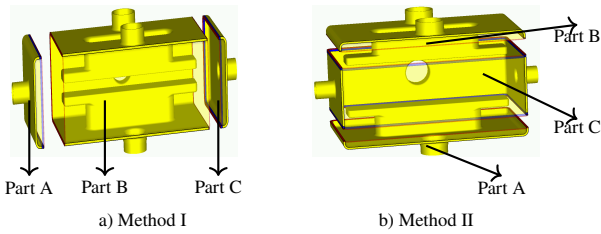


Figure 2: The cavity is divided into three parts in the two different methods considered for fabricating the cavity.

was divided into three parts taking these constraints into account. Primarily, the deflecting cavity can be divided into two ways for fabrication (Fig. 2).

In the first method, the stems are machined to the exact dimensions using a single block to form Part B, whereas parts A and C are machined separately with excess height where they join with Part B (Fig. 2 a). This method is similar to the fabrication methodology followed in machining the superconducting deflecting cavity discussed in [4]. The excess material from parts A and C can be trimmed for the frequency pre-tuning of the cavity, and this excess height has a frequency sensitivity of  $-93.51$  kHz/mm in the present cavity. In the second method, parts A and B are machined separately from different copper blocks with higher precision. On the other hand, Part C may have extra height where it meets parts A and B. In the present deflecting cavity, the trimming of additional height has a frequency sensitivity of  $2.76$  MHz/mm.

A lower sensitivity value for the trimming region allows for precise tuning of the cavity frequency. In this context, Method I is preferable, but this demands long milling tools to reach the center of Part B. A longer tool tends to flex, causing shudder and overloading of the milling spindle. A tool with larger diameter will avoid shuddering, but this degrades the surface quality. Even though Method II requires precise trimming and a superior brazing quality, the most sensitive parts of the cavity, the stems, can be machined to higher precision. Method II was eventually chosen, with an accuracy of  $40\ \mu\text{m}$  defined for trimming the excess height from Part C.

The three cavity parts were machined from a copper block (Fig. 3). An additional stainless steel fixture functioned as a template for aligning the cavity parts during machining (Fig. 3 d). This helped reach the specified dimensional tolerances. The dimensions of the machined parts were measured and verified against the design values. In addition, the root mean square surface roughness was measured at different points on the cavity's inner surface. The measured values ranged from  $0.3\ \mu\text{m}$  to  $2\ \mu\text{m}$ , which was significantly lower than the specified value of  $3\ \mu\text{m}$ .

## FREQUENCY PRE-TUNING

Despite the fact that the cavity parts were machined with great accuracy, fabrication errors cannot be totally eliminated. Fabrication errors intrinsically change the cavity geometry and affect the cavity's resonance frequency. This

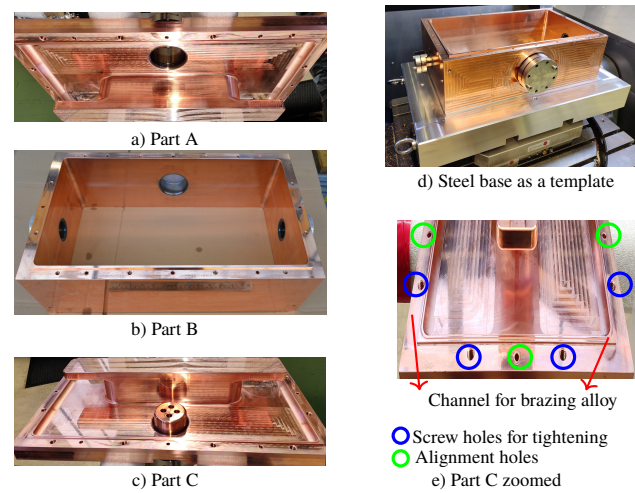


Figure 3: Three parts of the copper cavity were machined separately, and the stainless steel base was used as a template for machining the parts.

frequency shift should be measured and corrected before the final brazing of the cavity parts. The Part C of the cavity had an excess height of  $5$  mm, and this increased the cavity aperture ( $v_{ap}$ ) to  $35$  mm, which also increased the frequency by  $12$  MHz. The cavity's resonance frequency for different cavity apertures obtained through simulation is shown in Fig. 4, and the data points are fitted to a quadratic function.

The trimming of the excess height of Part C decreases both the cavity aperture and the resonance frequency. Subsequently, three data points were considered sufficient for extrapolating a quadratic curve, and three machining steps were chosen. Before every machining step, the cavity sections were stacked, lined up with the aid of the alignment holes and bolted to achieve leak-tight joints (Fig. 3 e). Then the distance between the stems (cavity aperture) and the cavity's resonance frequency was measured. Importantly,

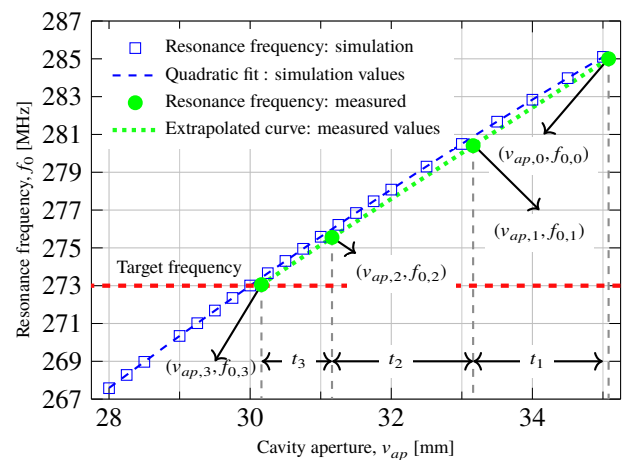


Figure 4: The cavity's resonance frequency for different apertures obtained from the simulation is plotted along with the values measured during the frequency pre-tuning process.

Table 2: Measurement Values Obtained During the Frequency Pre-tuning of the Cavity

Step	Trim	Aperture $v_{ap}$ [mm]		Frequency $f_0$ [MHz]	
	t [mm]	Expected	Measured	Expected	Measured
0 <sup>th</sup>	–	35.08	35.08	285.237	285.002
1 <sup>st</sup>	2.00	33.08	33.16	280.830	280.407
2 <sup>nd</sup>	2.00	31.16	31.16	275.966	275.554
3 <sup>rd</sup>	0.98	30.18	30.16	273.000	273.056
After brazing		30.16	30.20	273.056	273.122

all the cavity components were installed to ensure that the pre-tuning process would also compensate for errors arising from these components. A trim height ( $t$ ) of 2 mm was fixed for the first two machining steps to ensure that there was sufficient excess material left for the final machining step. The results of the frequency pre-tuning are given in Table 2 and Fig. 4, and the cavity resonance frequency was offset only by +56 kHz. After that, vacuum brazing of the cavity was carried out, and this increased the frequency error by 62 kHz. This frequency shift can be compensated easily with the available frequency tuners.

The intrinsic quality factor of the cavity ( $Q_0$ ) after brazing was measured to be 6500, which was 60 % of the design value. A decrease in  $Q_0$  by half doubles the RF power required to achieve a required kick voltage. Therefore, it was important to investigate the degradation of the quality factor in the present case.

## INVESTIGATION OF LOW $Q_0$

The intrinsic quality factor of the cavity not only depends on the power loss on the plain cavity surface but also on the frequency tuners, the fundamental power coupler (FPC), the pick-up probe and the RF filter at the vacuum port. Thus, each of these losses must be measured independently to determine the element that lowers the  $Q_0$ . The Q-factor of the individual components is measured one at a time using the two loosely coupled antennae placed at the Port 1 and Port 2, i.e., at the beam entrance and exit of the cavity. The Q-factor of the cavity components obtained during measurement is compared with the simulation in Table 3. Besides the RF filter, the measured Q-factor agrees with the simulated results.

In the pre-buncher cavity at ELBE, a rectangular steel mesh securely fastened to a steel cup was used to prevent a leak in the RF field via Port A. A similar concept was emulated in the present cavity. The low conductivity steel mesh and improper electrical contact increased the surface resistance, resulting in a higher Q-factor. Originally, the RF filter was provided to prevent field leakage to the vacuum pump. As the operating frequency is an order lower than the cut-off frequency of Port A (2.791 GHz), the field will significantly decay before it reaches the other end of the port. As a result, the RF filter was not used, and a  $Q_0$  of 10250 was measured.

Table 3: The Q-factor of the individual cavity components obtained from the measurement is compared with the simulation.

Port	Component	Q-factor from	
		measurement	simulation
–	Cavity	10 465	10 741
A	RF filter	19 506	$6.27 \times 10^5$
B	Pick-up	$5.98 \times 10^5$	$6.93 \times 10^5$
C	FPC	$5.88 \times 10^5$	$2.26 \times 10^6$
D	Tuner 1	$6.24 \times 10^5$	$8.25 \times 10^5$
E	Tuner 2	$6.24 \times 10^5$	$7.96 \times 10^5$

## FIELD MEASUREMENT

The perturbation of a cavity by a small bead shifts the resonance frequency, and the change in resonance frequency is proportional to the field at the perturbing object [5]. A bead-pull measurement setup was built similar to the one discussed in [6]. The dielectric and metallic spherical beads of 5 mm diameter were used for measurements. As the bead travels along the cavity axis, it perturbs the field, and the input signal's phase shift at the resonance frequency was recorded. The phase shift  $\Delta\phi$  is converted to the frequency shift  $\Delta\omega$  using the expression:

$$\frac{\Delta\omega}{\omega} = \frac{1}{Q_0} \tan \Delta\phi. \quad (1)$$

Figure 5 shows the results of the bead-pull measurement. Here, the frequency shift obtained with the dielectric sphere directly corresponds to  $E_y$ . In contrast, the influence of  $H_x$  has to be extracted from the values measured with the metallic bead [6]. Therefore, the dielectric field result was scaled such that the values obtained at the cavity center ( $z = 0$ ) were identical to those of the metallic sphere. Subsequently, the difference between the metallic and scaled dielectric values renders  $|H|^2$ . This procedure is justified, since in the center of the cavity at  $z = 0$  only an electric field exists and thus both a dielectric and a metallic bead must give the same result. Qualitatively, the field profiles obtained from the bead pull measurement agree with the simulation results.

## RF TEST SETUP

After the field measurement, the cavity was cleaned to ISO 5 cleanroom standards. An experimental setup was built to conduct the warm RF testing of the cavity (Fig. 6). A signal generator drives the RF amplifier, and the power is delivered to the cavity via a circulator, which protects the amplifier from the reflected power. Power meters are used to measure the input power, the reflected power and the power sampled by the pick-up probe. A temperature-controlled chiller provides cooling water required for the cavity, FPC, amplifier and circulator.

The cavity was evacuated, and a base pressure of  $6 \times 10^{-9}$  mbar was reached. The input power to the cavity was increased in steps after ensuring a stable vacuum at

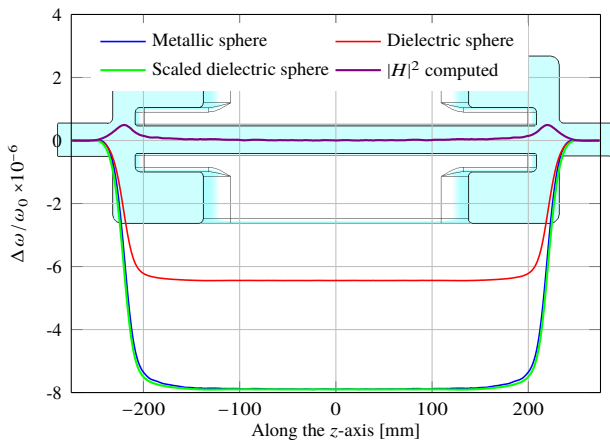


Figure 5: The relative frequency change along the cavity axis measured with the metallic and the dielectric spherical bead. The graph represents the mean of 40 measurements, and the difference between the values of the scaled dielectric and those of the metallic sphere render  $|H|^2$ .

each step. At 400 W of input power, the temperature on the surface of the pick-up probe increased to 67 °C (Fig. 7 a). The surface power loss on the pick-up is high due to the low electrical conductivity of the steel. Furthermore, absence of cooling channels in this region resulted in poor heat conduction which increased its surface temperature. The input power to the cavity was not increased further to avoid damaging the pick-up probe.

Installation of the coolant channels on the existing pick-up was technically not possible. Therefore, the inner surface of the pick-up cup was coated with silver (Fig. 7 b), which in-

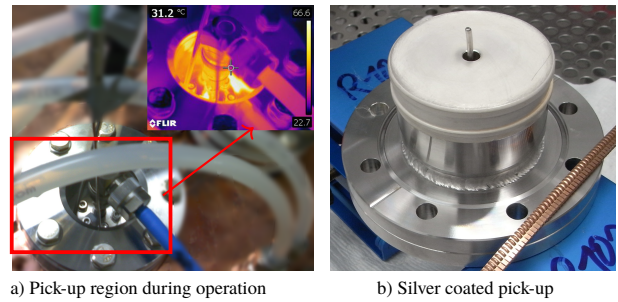


Figure 7: A snapshot of the pick-up probe surface captured through an infrared camera when 400 W of power was fed to the cavity (a) and the silver coated pick-up cup (b).

creased the electrical conductivity, lowering the surface loss. By this, the cavity was successfully vacuum conditioned at 1 kW with the modified pick-up probe. At this power level, the temperature on the pick-up surface was around 45 °C.

## SUMMARY

A copper prototype deflecting cavity required for the beam separation at ELBE has been successfully fabricated. Degradation of the intrinsic quality factor was investigated, and elimination of the RF filter improved the Q-factor. Furthermore, the field profile along the cavity axis was measured, and the results agree with the simulation. An RF test setup was built, and the cavity was vacuum conditioned with the modified pick-up. The cavity meets the design requirements and is ready to be tested with a beam.

## REFERENCES

- [1] P. Michel, “ELBE center for high-power radiation sources,” *J. Large-Scale Res. Facil.*, vol. 2, p. A39, 2016. doi:10.17815/jlsrf-2-58
- [2] G. T. Hallilingaiah, A. Arnold, U. Lehnert, P. Michel, and U. van Rienen, “Numerical Studies of Normal Conducting Deflecting Cavity Designs for the ELBE Accelerator,” in *Proc. IPAC’18*, Vancouver, Canada, Apr.-May 2018, pp. 3824–3827. doi:10.18429/JACoW-IPAC2018-THPAL074
- [3] P. Evtushenko, “Novel high repetition rate CW SRF LINAC-based multispectral photon source,” in *Proc. IPAC’22*, Bangkok, Thailand, Jun. 2022, pp. 1427–1430. doi:10.18429/JACoW-IPAC2022-TUPOMS013
- [4] D. W. Storey, R. E. Laxdal, B. Matheson, and N. Muller, “Fabrication Studies of a 650 MHz Superconducting RF Deflecting Mode Cavity for the ARIEL Electron Linac,” in *Proc. IPAC’17*, Copenhagen, Denmark, May 2017, pp. 120–122. doi:10.18429/JACoW-IPAC2017-MOPAB022
- [5] L. C. Maier and J. C. Slater, “Field strength measurements in resonant cavities,” *J. Appl. Phys.*, vol. 23, no. 1, pp. 68–77, 1952. doi:10.1063/1.1701980
- [6] M. Navarro-Tapia and R. Calaga, “Bead-Pull Measurements of the Main Deflecting Mode of the Double-Quarter-Wave Cavity for the HL-LHC,” in *Proc. SRF’15*, Whistler, BC, Canada, Sep. 2015, pp. 1105–1109. doi:10.18429/JACoW-SRF2015-THPB019

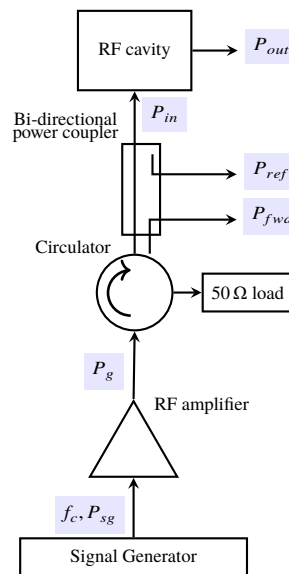


Figure 6: The cavity and the associated components arranged for the warm RF test (left); the sketch shows the RF devices and the power measurement points.

Content from this work may be used under the terms of the CC BY 4.0 licence (© 2021). Any distribution of this work must maintain attribution to the author(s), title of the work, publisher, and DOI